

High Order Modes in Project-X Linac

A. Sukhanov*, A. Lunin, V. Yakovlev, M. Awida, M. Champion,
C. Ginsburg, I. Gonin, C. Grimm, T. Khabiboulline, T. Nicol, Yu. Orlov,
A. Saini, D. Sergatskov, N. Solyak, A. Vostrikov

Fermilab, Batavia, IL 60510, USA

Abstract

Project-X, a multi-MW proton source is now under development at Fermilab. In this paper we present study of high order modes (HOM) excited in continuous-wave (CW) superconducting linac of Project-X. We investigate effects of cryogenic losses caused by HOMs and influence of HOMs on beam dynamics. We find that these effects are small. We conclude that HOM couplers/dampers are not needed in the Project-X SC RF cavities.

Keywords: superconducting proton linac, high order modes, beam dynamics

1. Introduction

Fermilab is currently developing a multi-MW proton source, Project-X (PX) [1], which will provide intense muon, kaon, neutrino and nuclei beams for broad and diverse program at the intensity frontier of particle physics. PX will allow study of applications of proton accelerators for energy production and nuclear waste transmutation in accelerator-driven subcritical systems. And, eventually, Project-X may become an integral part and driver for the future Fermilab Neutrino Factory and/or Muon Collider. Figure 1 shows a general layout of Project-X.

A key component of Project-X is the CW SRF linac, which accelerates bunches of $\sim 16 \cdot 10^7$ H^- ions from 2.1 MeV to 3 GeV. The linac layout

*ais@fnal.gov

¹Operated by Fermi Research Alliance, LLC under Contract No. De-AC02-07CH11359 with the United States Department of Energy.

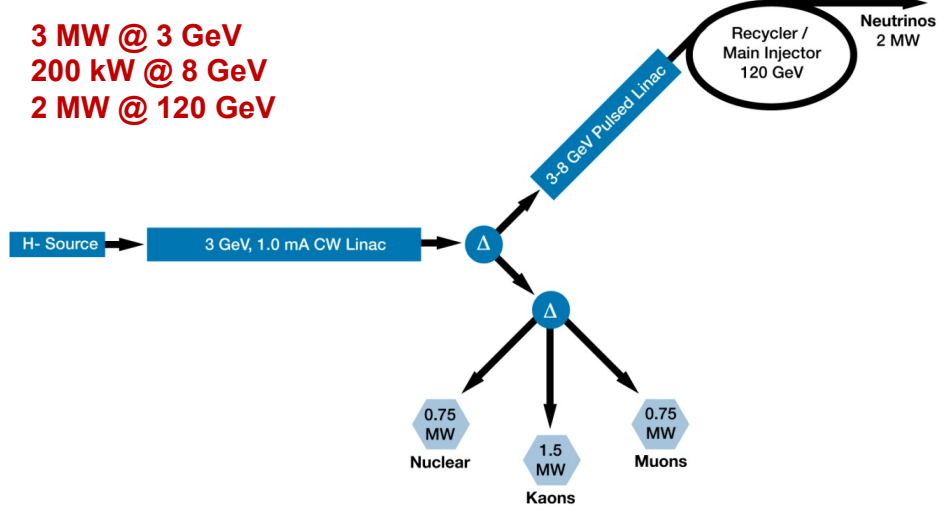


Figure 1: Project-X layout.

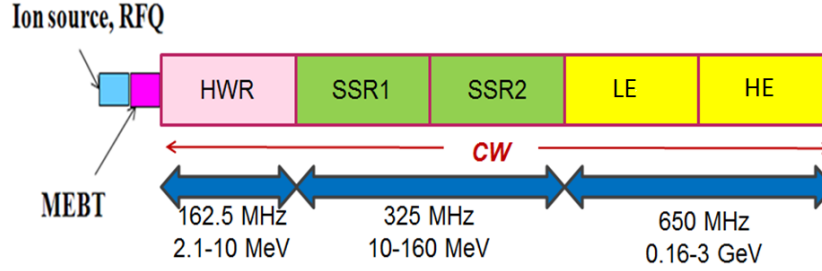


Figure 2: Layout of Project-X CW linac.

12 is shown in Figure 2. It includes a section of half-wave resonators (HWR,
 13 Figure 3a) at 162.5 MHz, two sections of single-spoke cavities (SSR1, Fig-
 14 ure 3b, and SSR2, Figure 3c) at 325 MHz, and low energy (LE) and high
 15 energy (HE) sections of 5-cell elliptical cavities at 650 MHz (see Figure 4).
 16 Two designs exist for the LE section, one from JLab [3] and one from Fer-
 17 milab [4]. The Fermilab design has been used for the calculations in this
 18 paper. The conclusions of this paper are not expected to vary significantly
 19 between two design. Table 1 lists nominal beam velocity β_G , energy range,
 20 total number of cavities, number of focusing magnets and number of cry-
 21 omodules (CM), length of cryomodules, and proposed packaging of cavities

22 and magnets inside cryomodules.

Table 1: Cavities and cryomodules in Project X linac.

Section	β_G	Freq. MHz	Energy MeV	Cav/Mag/ CM	Type of cavities, magnets, CM length
HWR	0.11	162.5	2.1–10	8/8/1	HWR, solenoid, 5.26 m
SSR1	0.22	325	10–32	16/8/2	SSR, solenoid, 4.76 m
SSR2	0.47	325	32–160	36/30/4	SSR, solenoid, 7.77 m
LE 650	0.61	650	160–520	42/14/7	5-cell ellip., doublet, 7.1 m
HE 650	0.9	650	520–3000	152/19/19	5-cell ellip., doublet, 11.2 m

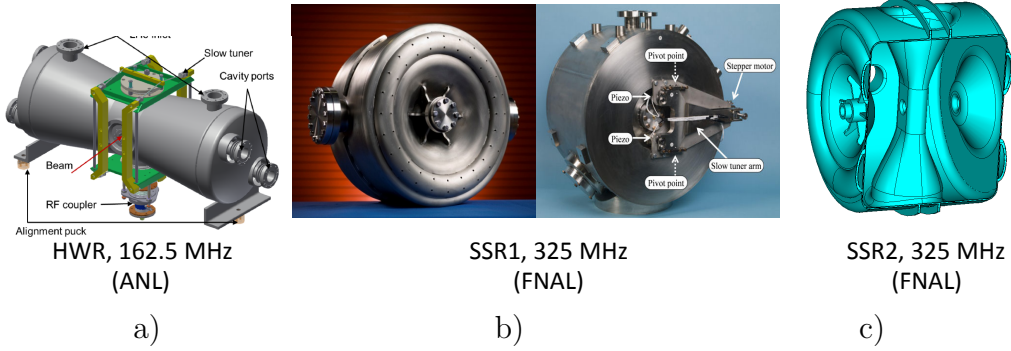


Figure 3: a) Half-wave, b) single spoke 1 (bare and dressed), and c) single spoke 2 cavities of Project-X.

23 RF design parameters of half-wave and single-spoke resonators are listed
 24 in Table 2. Table 3 presents RF design parameters of the both LE and HE
 25 650 MHz cavities. In these tables parameter G is cavity *geometry constant*
 26 (see, for example, [2], p. 45, eq. 2.52). Parameters E_{acc} , (R/Q) ,² that depend
 27 on beam velocity β , are shown for the optimal velocity, β_{opt} . Intrinsic quality
 28 factor Q_0 and heat load are given at 2 K.

29 1.1. Importance of HOM investigation

30 Excitation of high order modes in SRF cavities is always a concern. Heat-
 31 ing caused by beam power lost to HOMs adds to the cryogenic losses and

²Note, that in this paper we use *accelerator* definition of (R/Q) value, as in [2], p. 47.

Table 2: Half-wave and single-spoke resonator cavities.

Type	Beam pipe \varnothing , mm	$\max V_{acc}$ MeV	$\max E_{acc}$ MV/m	B_{\max} mT	(R/Q) Ω	G Ω	Q_0 $\times 10^{10}$
HWR	33	1.8	40	62	225	47.7	1.0
SSR1	30	1.95	28	70	242	84	1.1
SSR2	40	3.34	32	60	292	109	1.3

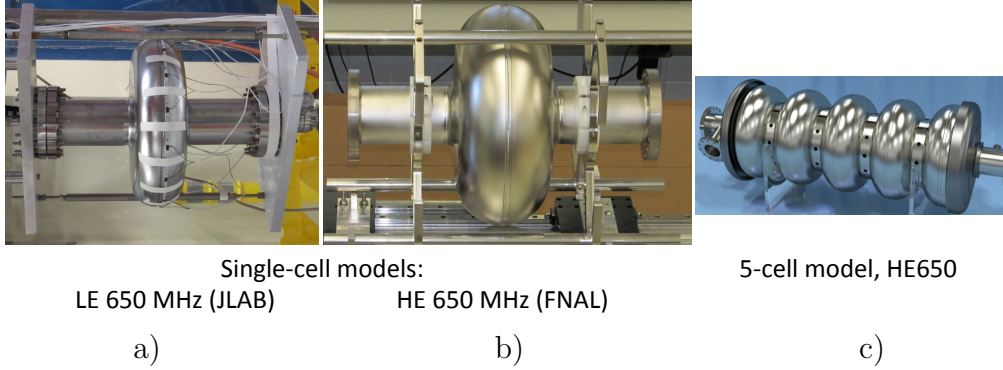


Figure 4: Elliptical cavities in Project-X linac: a) LE 650 MHz single-cell prototype cavity (JLab design); b) HE 650 MHz single-cell prototype cavity (Fermilab design); and c) HE 650 MHz 5-cell prototype cavity.

increases operational cost of the linac. Interaction of the beam with excited HOMs deteriorates the quality of the beam.

One of the ways to reduce HOMs is to equip accelerating cavities with couplers, which re-direct and dump HOMs outside of the cavities. The drawback of this solution is that the HOM couplers are vulnerable, expensive, and complicated part of the SC accelerating structure and not effective in the full range of the HOM frequencies. HOM couplers add extra hardware to cryomodules: cables, feed-through, connectors, loads, *etc.* They are susceptible to multipactoring and damage of feed-throughs.

Experience with super-conducting proton linac at SNS shows that HOM couplers may limit cavity performance and reduce operation reliability. Observed power loss to HOMs at SNS is very small and HOM couplers were found to be not necessary [5].

Power loss to HOMs and, respectively, their adverse effect on beam quality and heat load depend on the beam current, beam spectrum, and the

Table 3: 650 MHz elliptical cavities.

Parameter	Units	LE 650	HE 650
β_G		0.61	0.9
L_{cav}	mm	703	1038
(R/Q)	Ω	378	638
G	Ω	191	255
$\max V_{\text{acc}}$	MeV	11.7	17.7
E_{acc}	MV/m	16.6	17
$\max E_{\text{surf}}$	MV/m	37.5	34
$\max B_{\text{surf}}$	mT	70	61.5
Q_0	$\times 10^{10}$	1.5	2.0
Maximum heat load	W	24	24

Table 4: Incoherent HOM power loss in Project-X, SNS and ILC.

	Project-X	SNS	ILC
I_{av} , mA	1	1	0.048
Q_b , pC	25.6	58	3200
k_{loss} , V/pC	2	1.1	13.4
P_{av} , mW/cavity	51	64	2065

47 cavity HOM spectrum. Assuming that each beam bunch excites HOMs in
 48 cavities independently from the other bunches (“incoherent losses”) an aver-
 49 age HOM power per cavity can be estimated as following: $P_{\text{av}} = k_{\text{loss}} q_b I_{\text{av}}$,
 50 where k_{loss} is a loss-factor, q_b is a bunch charge, and I_{av} is an average beam
 51 current. Table 4 compares incoherent losses in Project-X, SNS, and ILC su-
 52 perconducting RF structures. One can see that in the ILC linac the HOM
 53 power loss is very high hence HOM dampers are necessary. All the 1.3 GHz
 54 ILC cavities are equipped with HOM couplers, that reduce loaded quality
 55 factors of longitudinal and transverse HOMs to 10^5 and work successfully at
 56 DESY. However, some problems with HOM couplers were encountered dur-
 57 ing long pulse operation [6]. In the SNS cavities no measurable HOM signals
 58 from beam were observed. Also, analysis of collective beam effects in SNS,
 59 such as a beam break-up and a klystron-type instability, do not show critical
 60 influence of high order modes on the beam dynamics [5].

1.2. Scope of investigation

The goal of this paper is to understand the HOM effects on the heat load and the beam dynamics in the Project-X superconducting RF cavities, and to decide whether HOM dampers are needed in the high and low energy sections of the CW linac. We focus our investigation on the following topics: calculation of loss factors (Section 2); investigation of beam spectrum for different modes of operation of Project-X (Section 3); simulation and measurement of cavity spectrum for all sections of linac (Section 4); estimation and measurement of spread of HOM frequencies and impedances; estimation of cryogenic loss taking into account non-propagating and propagating modes; estimation of the longitudinal and transverse beam emittance dilution caused by HOMs (Section 5); investigation of stability of HOMs with respect to tuning and detuning of the accelerating mode (Section 6); estimation of longitudinal and transverse beam instabilities (Section 7); comparison to the existing proton superconducting linacs (SNS); study of effects of microphonics for different HOMs (Section 8.1).

Project-X has complicated beam timing structure. Beam current is rather small and beam is non-relativistic. Beam passes linac only once, so there is no feedback as in circular accelerators. All the above factors affect excitation of high order modes.

2. Incoherent losses

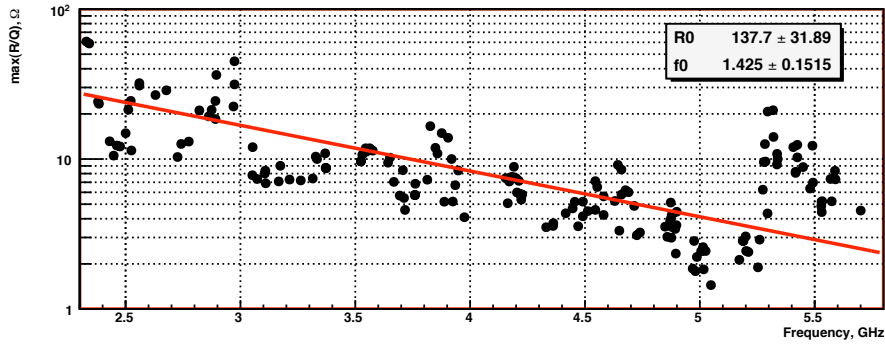


Figure 5: Impedance of longitudinal HOMs in HE 650 MHz section of Project-X calculated with SuperLANS. Data are approximated by an exponential function $(R/Q) = R_0 \exp(-f/f_0)$, with $R_0 = 137.7 \Omega$, and $f_0 = 1.425$ GHz.

82 We use SuperLANS [7] program³ to calculate spectrum of HOMs in HE
83 650 MHz sections of Project-X. The cavity model and geometry are described
84 in more details in Section 4.1. In general, modes with the frequencies above
85 the beam pipe cut-off frequency⁴ escape, or propagate from the cavity into
86 beam pipe and can be removed from the accelerator by HOM couplers and
87 absorbers. But when multiple cavities are put together in a linac at the
88 regular intervals, conditions may arise where some of these modes are effec-
89 tively trapped inside the cavity chain. Without experimental data from real
90 linac or a complete model of entire accelerator it is not possible to predict
91 which of the propagating modes may be trapped. We use a conservative
92 approach and assume that all propagating modes are trapped. Impedance of
93 propagating modes depends on the length of the beam pipe between adjacent
94 cavities. In our calculations we model single cavity with beam pipes attached
95 at the cavity ends. The beam pipes are closed with perfect electric conductor
96 (PEC) flanges. We vary length of the beam pipes in the range from 10 to
97 50 cm in increments of 1 mm and calculate cavity spectrum for each length.
98 We then use the maximum value of impedance of the propagating modes
99 with respect to the beam pipe length. Figure 5 shows frequency dependence
100 of the impedance of the longitudinal HOMs. The impedance quickly drops
101 with the frequency and can be approximated by an exponential function:
102 $(R/Q) = R_0 \exp(-f/f_0)$ with $R_0 = 137.7 \Omega$ and $f_0 = 1.425$ GHz, f is the
103 HOM frequency.

104 The effect of beam velocity on HOMs can be demonstrated using the
105 following consideration (see Figure 6). Frequencies (and number) of HOMs
106 excited by a beam bunch, passing through an SRF structure, depend on the
107 characteristic size of the EM field distribution on the wall of the beam pipe at
108 the cavity entrance, σ_{field} . In linacs with relativistic beam, such as ILC [8],
109 XFEL [9] or NGLS [10], the field distribution is essentially disk-like and
110 $\sigma_{\text{field}} \sim \sigma_{\text{bunch}}$. Bunch EM field spectrum has frequencies up to $f_{\text{max}} \sim$

³SuperLANS is fast and simple program which allows for quick finding of monopole, dipole and quadrupole eigen-modes in axially symmetric RF structures.

⁴The beam pipe cut-off frequency the lowest frequency of the beam pipe waveguide modes. The lowest propagating TM mode of the cylindrical beam pipe of radius a has the cut-off frequency $f_{\text{cut-off}} = \frac{ct_{01}}{2\pi a}$, where c is speed of light and $t_{01} \approx 2.4048$ is the 1st zero of Bessel function of 0th order: $J_0(t_{01}) = 0$. For example, HE 650 MHz section of Project-X linac has the beam pipe of radius $a = 5$ cm and the cut-off frequency $f_{\text{cut-off}} \approx 2.3$ GHz.

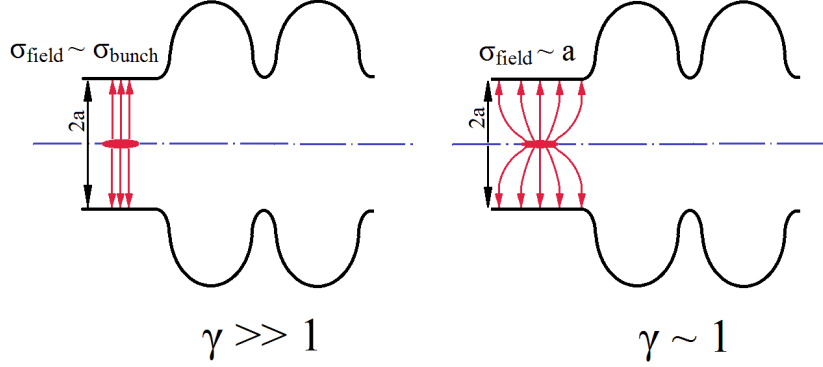


Figure 6: Effect of beam velocity on HOM excitation.

111 c/σ_{bunch} . For the bunch size of $50 \mu\text{m}$ $f_{\text{max}} = 6 \text{ THz}$. In case of a non-
 112 relativistic beam, field lines diverge much more, and the characteristic size
 113 of field distribution is of the order of the beam pipe radius, $\sigma_{\text{field}} \sim a$ and
 114 $f_{\text{max}} \sim c/a$. If the beam pipe radius is 50 mm , only frequencies below 6
 115 GHz are present in the bunch field spectrum. Taking into account rapid
 116 exponential decay of HOM spectrum as shown in Figure 5, we conclude
 117 that effectively only HOMs below few GHz will be excited by the non-
 118 relativistic beam in the Project-X linac.

119 We perform simulation of incoherent losses using time-domain calcula-
 120 tions [11] in CST Studio program [12]. Results are shown in Figure 7. Losses
 121 are well below 100 mW/cavity in HE 650 MHz section, and of the order of
 122 magnitude smaller in LE 650 MHz part.

123 3. Beam spectrum

124 Amplitude and frequency of the main lines of the beam current spectrum
 125 directly affect probability of excitation and strength of high order modes in
 126 superconducting accelerating RF structures.

127 The bunch sequence frequency in Project-X is 162.5 MHz . A broad-band
 128 chopper provides the beam structure needed for the experiments. Three
 129 regimes of operation are considered:

- 130 1. A bunch timing structure required for muon, kaon, and nuclear experi-
 131 ments at 3 GeV . Figure 8 shows one full period (approximately $1 \mu\text{s}$) of
 132 the bunch train in this regime. Average beam current is 1 mA . The de-

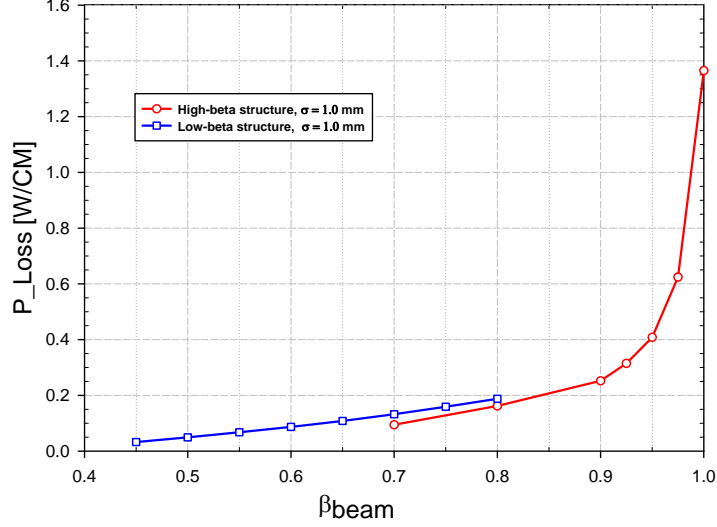


Figure 7: Incoherent losses per cryomodule in LE and HE 650 MHz sections of Project-X linac.

- livered power is 700/1540/770 kW for muon/kaon/nuclear experiments, respectively.
2. A 3 GeV structure combined with 10 Hz 5% duty factor (DF) pulses for injection into the Fermilab Main Injector (MI) for the 120 GeV neutrino program; 33% of the bunches within pulses are removed to match the phase of ~ 50 MHz of MI RF.
 3. A 3 GeV structure combined with 15 Hz 10% DF pulses, which can be used to drive a future Muon Collider; within these pulses, bunches are structured in $1 \mu\text{s}$ “micro”-pulses with a 50% DF. The mean value of pulsed current in this mode is 5 mA.

The spectrum for an idealized 3 GeV beam structure, assuming very short bunches of equal charge and the absence of timing jitter, is shown in Figure 9. The main lines are harmonics of 162.5 MHz, 20 MHz and 10 MHz corresponding to the three components of the beam for muon, kaon and nuclei experiments. The sideband lines of 1 MHz quickly fall below 0.1 mA.

Because of the small duty factor of 5% and chopping off 33% of bunches during the MI pulses in the mode 2, there are only very minor modifications

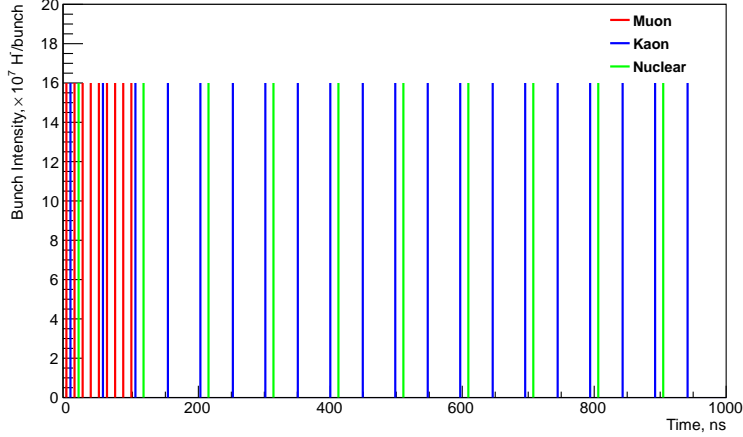


Figure 8: Beam structure for 3 GeV program.

to the beam current spectrum of the 3 GeV timing structure. Indeed, in this case, 10 Hz sidebands are added to 1 MHz lines of the 3 GeV spectrum shown in Figure 9. The amplitude of these lines falls quickly from 0.1 mA to the sub- μ A level. Since we are already considering variations of HOM frequencies of the order of 1 MHz, the effect of MI pulses on the power loss is negligible.

The spectrum of the beam current corresponding to the pulses for Muon Collider operation is shown in Figure 10. The main lines of this spectrum are the harmonics of the bunch sequence frequency, 162.5 MHz, with an amplitude of about 1 mA⁵. The amplitude of the sideband lines, separated by 2 MHz (due to 50% DF during the “micro”-pulse), drops quickly below 0.1 mA.

4. Cavity spectrum

In this section we evaluate spectra and impedances of the high order modes in the Project-X cavities. The main contribution into HOM losses comes from the modes with the highest impedance and the ones with the frequencies in proximity of the main lines of beam current spectrum.

⁵Note that the average value of pulsed current is 5 mA, but there is a 10% pulse DF and 50% DF at the 1 μ s “micro”-pulse level.

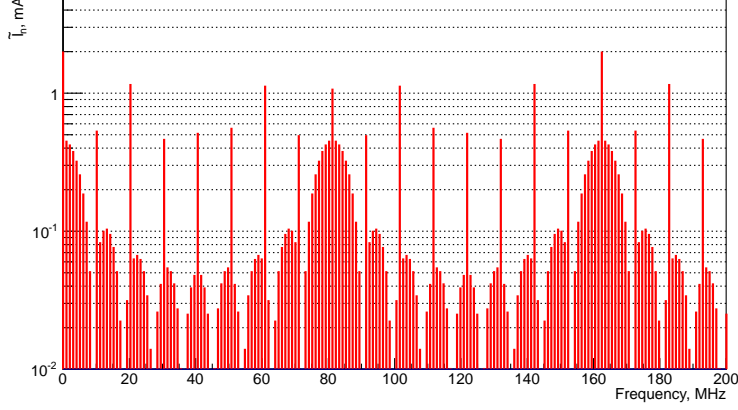


Figure 9: Beam spectrum of 3 GeV program.

167 4.1. 650 MHz cavities

168 Figure 11 shows a parameterization of geometry of the half-cell of an
 169 elliptical cavity. There is rotational symmetry with respect to the cavity
 170 axis (side L on Figure 11). The full accelerating cavity is made of few cells
 171 that may have different geometry in order to achieve better field flatness on
 172 the cavity axis. Parameters of half-cells of 650 MHz Project-X cavities for
 173 $\beta = 0.6$ and $\beta = 0.9$ are shown in Table 5. The full cavity is made of five
 174 cells. Attached to the both sides of the cavity is the beam pipe of the radius
 175 r from Table 5. Length of the beam pipe is a variable parameter in field
 176 calculations.

177 Results of spectrum calculation of 650 MHz cavities using SuperLANS
 178 code and PEC boundary conditions at the beam pipe ends are shown in
 179 Figure 12 for non-propagating monopole modes and in Figure 13 for dipole
 180 HOMs. Figure 14 and Figure 15 show impedances of the same modes.⁶ One
 181 can observe, that all monopole HOMs in LE 650 MHz section have impedance

⁶We use the following definition of the dipole mode impedance:

$$\left(\frac{R}{Q}\right)^{(1)} = \frac{\left|\int (\nabla \perp E_z)|_{x=x_0} e^{i\omega z/v} dz\right|^2}{W\omega},$$

where ω is the mode circular frequency, W is stored energy, v is beam velocity. The integral is taken along the line parallel to the cavity axis at the distance x_0 .

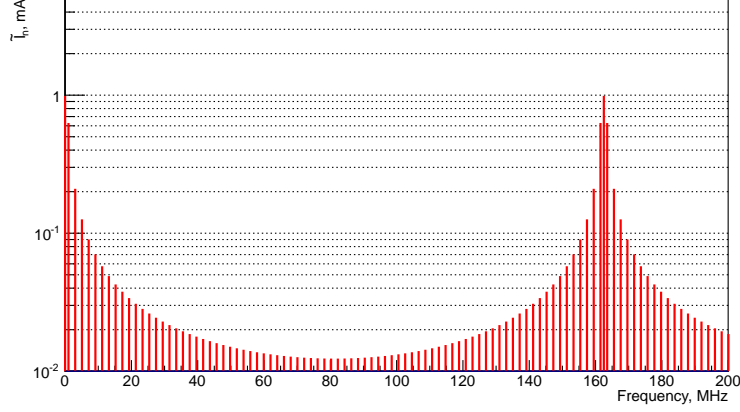


Figure 10: Beam spectrum of Muon Collider pulses.

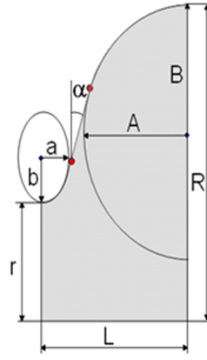


Figure 11: Parameterization of geometry of elliptical cavities.

below 10Ω . In HE 650 MHz section there are two monopole modes, with the frequencies of 1988 MHz ($\delta f = 2.2 \text{ MHz}$ ⁷) and 2159 MHz ($\delta f = 3.9 \text{ MHz}$) have impedance of 12Ω ; one mode with the frequency of 1238.6 MHz ($\delta f = 0.44 \text{ MHz}$) has impedance of 22Ω ; and one mode with the frequency of 1241.1 MHz ($\delta f = 2.0 \text{ MHz}$) has impedance of 130Ω . There are exist three dipole modes in LE 650 MHz cavities ($f = 974, 978.6$ and 1293 MHz) with impedance above $10^4 \Omega/\text{m}^2$; and four modes in HE 650 MHz section ($f =$

⁷Here δf is the difference between HOM frequency and the nearest main beam spectrum line

Table 5: Geometrical parameters of 650 MHz Project-X cavities.

Dimension	$\beta_G = 0.61$		$\beta_G = 0.9$	
	Regular Cell	End Cell	Regular Cell	End Cell
r , mm	41.5	41.5	50	50
R , mm	195	195	200.3	200.3
L , mm	70.3	71.4	103.8	107.0
A , mm	54	54	82.5	82.5
B , mm	58	58	84	84.5
a , mm	14	14	18	20
b , mm	25	25	38	39.5
α , °	2	2.7	5.2	7

946.6, 950.3, 1376 and 1383 MHz) with $(R/Q)^{(1)} > 10^4 \Omega/\text{m}^2$.

Since for a non-relativistic beam HOM impedance depends on beam velocity, we also calculated (R/Q) as a function of β . Figure 16 shows dependence of impedance on the beam velocity for the potentially dangerous monopole and dipole modes in HE 650 MHz cavities.

We will perform measurements of HOM spectra and impedances of 650 MHz cavities and compare them to the calculated results when 5-cell prototype cavities will become available at Fermilab later this year.

4.2. HWR and SSR cavities

The spectra of HWR and SSR cavities are quite sparse. The HOM impedances fall quickly with frequency and are of the order of few $\text{m}\Omega$ at frequencies above 2 GHz. We do not expect large HOM losses in these sections of the linac.

An extensive HOM analysis of SSR1 cavities including simulation of spectra and impedances of monopole, dipole, and quadrupole modes as well as measurements of spectra and R/Q values of monopole HOMs up to 2 GHz of six fabricated SSR1 resonators has been performed and presented in [13]. The calculated and measured values are found to be in a good agreement. The measured HOM frequency spread is within 7 MHz.

Simulation studies of SSR2 and HWR cavities, similar to these of SSR1 described above, have been started. We will report results soon.

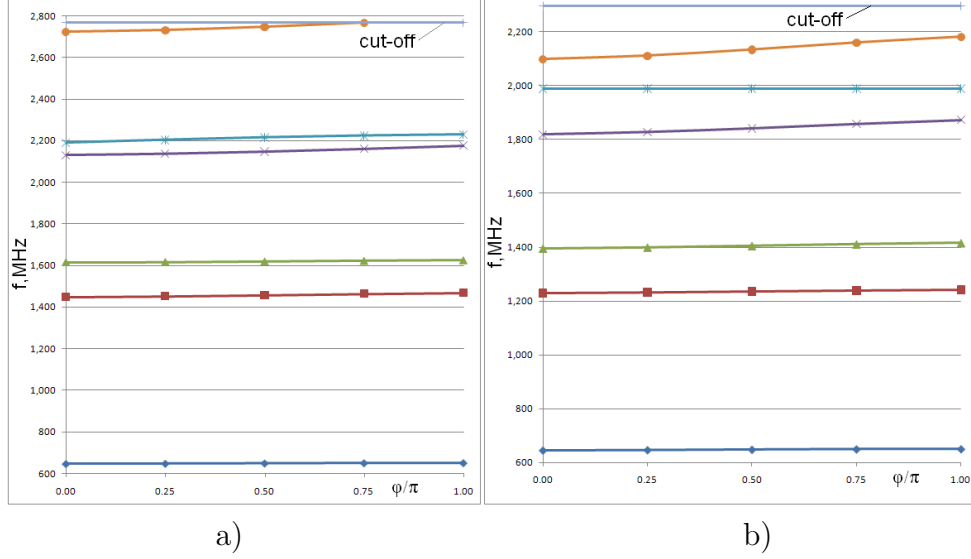


Figure 12: Spectrum of monopole HOMs in LE 650 (a) and HE 650 (b) sections of Project-X linac.

210 5. Resonance HOM excitation

211 A bunched continuous beam passing through a superconducting cavity
 212 may coherently excite cavity HOMs with high Q -factor, which are close to
 213 one of the beam spectrum lines. Here we present an estimations for the
 214 resonance excitation of the monopole and dipole high order modes in the HE
 215 part of the Project-X linac.

216 We require, that the monopole modes should not increase the longitudinal
 217 emittance of the beam, ε_z :

$$\sigma_{U_{HOM}} \sigma_z / c \ll \varepsilon_z, \quad (1)$$

218 where $\sigma_{U_{HOM}} = \frac{1}{\sqrt{2}} \hat{U}_{HOM}$ is the r.m.s. of energy gain caused by HOM with
 219 the amplitude \hat{U}_{HOM} , σ_z is a bunch length, and c is speed of light. For high- Q
 220 resonances one can get:⁸

$$\hat{U}_{HOM} \approx \frac{\tilde{I}(R/Q)}{4\delta f/f}, \quad (2)$$

⁸We use the following exact expression for the amplitude of HOM with frequency f and impedance (R/Q) excited by beam harmonic with amplitude \tilde{I} and frequency $f + \delta f$

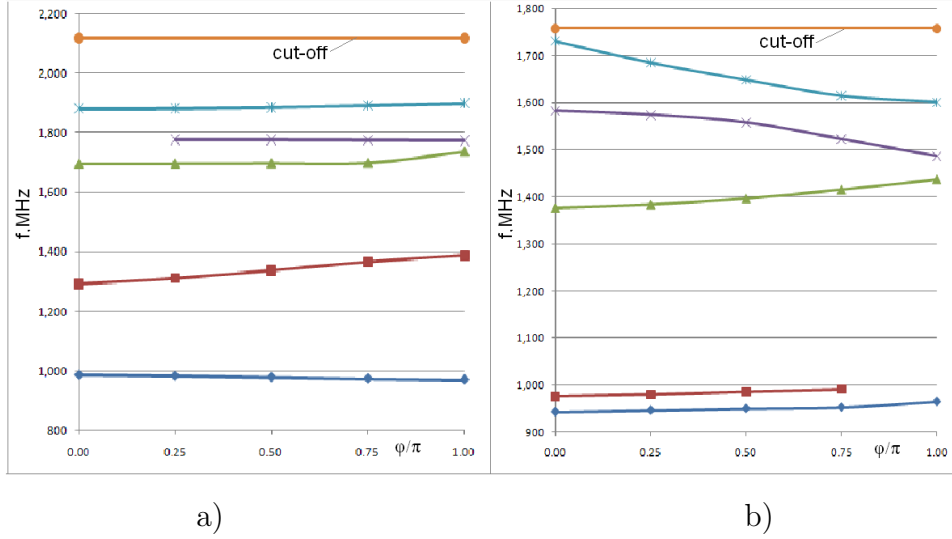


Figure 13: Spectrum of dipole HOMs in LE 650 (a) and HE 650 (b) sections of Project-X linac.

where \tilde{I} is the amplitude of a beam spectrum line, δf is the difference between the HOM frequency f and the beam spectrum line frequency. Here we assume that $\delta f/f \gg 1/Q$.

Finally, we obtain an estimation for the frequency detuning, δf , that does not lead to a longitudinal emittance growth:

$$\delta f \gg f \frac{\tilde{I}(R/Q)\sigma_z}{4\sqrt{2}\varepsilon_z c}. \quad (3)$$

We have the worst case at the start of the HE 650 MHz section, where the bunch length is at the maximum ($\sigma_z/c = 7.7 \times 10^{-3}$ ns), the second pass-band monopole HOM (1241 MHz and highest $R/Q = 130 \Omega$), the nearest large amplitude beam spectrum line ($\tilde{I} = 1$ mA), and the results from Eq. 3: $\delta f \gg 140$ Hz, obtained with the value of the emittance $\varepsilon_z = 1.5$ keV·ns [15]. Thus, if the distance between the beam spectrum lines is 1 MHz and the

(see, for example, [14]):

$$\hat{U}_{HOM} = -i \frac{f(f + \delta f)}{(f + \delta f)^2 - f^2 - i \frac{f(f + \delta f)}{Q}} \frac{\tilde{I}}{2} \left(\frac{R}{Q} \right).$$

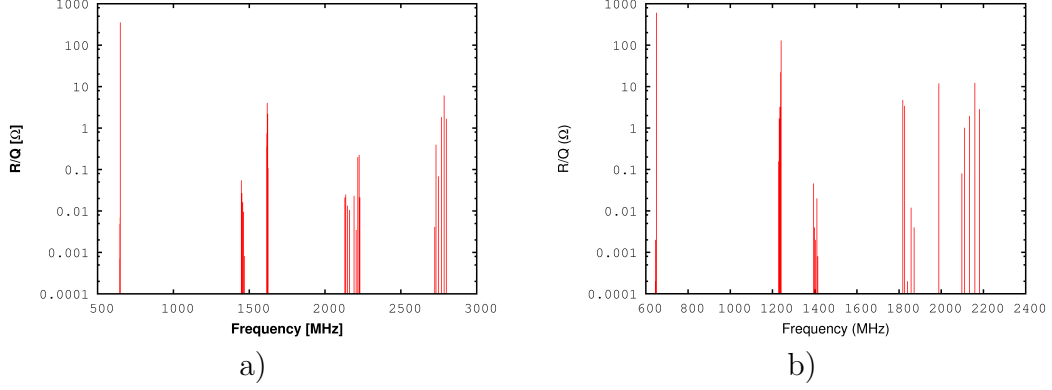


Figure 14: Impedance of monopole HOMs in LE 650 (a) and HE 650 (b) sections of Project-X linac.

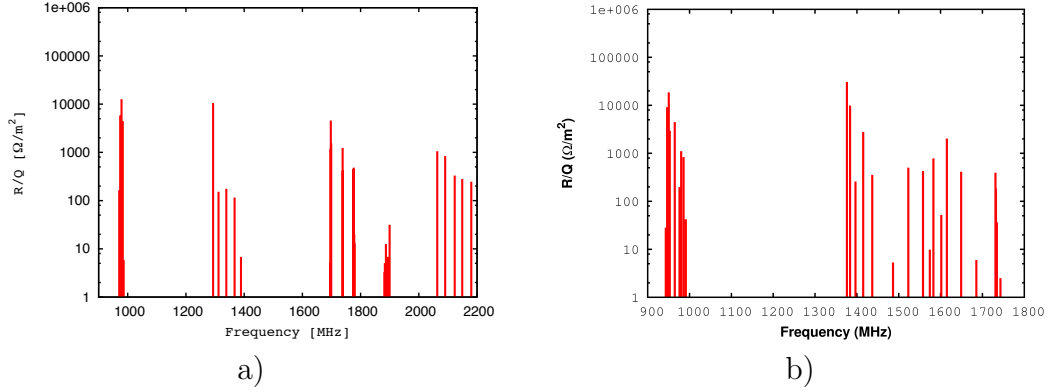


Figure 15: Impedance of dipole HOMs in LE 650 (a) and HE 650 (b) sections of Project-X linac.

monopole HOM frequency spread is about 1–2 MHz, the probability that the cavity has the resonant frequency close enough to the beam spectrum line is less than 10^{-4} for the baseline of the ProjectX CW linac.

The cryogenic losses are proportional to the square of the HOM field amplitude:

$$P_{loss} \approx \frac{\hat{U}_{HOM}^2}{(R/Q)Q_0}, \quad (4)$$

where Q_0 is an intrinsic quality factor. Therefore, it requires much close proximity of the beam spectrum line and HOM frequency in order to get significant cryogenic losses. If the HOM mode is exactly at the resonance, $U_{HOM} = \frac{1}{2}\tilde{I}(R/Q)Q_L$, where Q_L is the loaded quality factor of the mode.

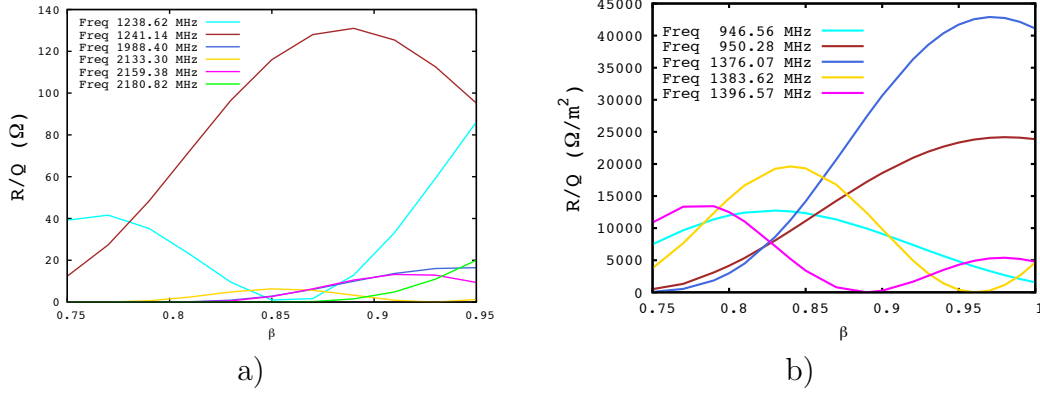


Figure 16: Impedance of the most dangerous monopole (a) and dipole (b) HOMs as a function of beam velocity β in HE 650 MHz cavities.

241 Requiring that P_{loss} is much smaller than the sum of the static heat load and
 242 the cryogenic losses due to accelerating mode (~ 20 W), and assuming that
 243 the intrinsic quality factor is $Q_0 = 5 \times 10^9$, we estimate that the maximum
 244 allowable value of the monopole HOM loaded quality factor is $Q_L \ll 6 \times 10^7$.

245 A similar approach can be employed for the analysis of dipole modes
 246 resonance excitation. The transverse kick caused by an HOM is:

$$U_{kick} \approx \frac{f}{4\delta f} \left(\frac{x_0}{k} \right) \tilde{I}(R/Q)^{(1)}, \quad (5)$$

247 where x_0 is the transverse offset of the beam trajectory, $k = 2\pi/\lambda$ is the
 248 wave number, and $(R/Q)^{(1)}$ is the transverse impedance (see definition in
 249 Section 4.1). Transverse emittance increase $\delta\epsilon_t$ may be estimated in the
 250 following way:

$$\delta\epsilon_t \approx \Delta x' \sigma_x = \frac{U_{kick}}{\sqrt{2}p_{\parallel}c} \sqrt{\epsilon_t \beta_f}, \quad (6)$$

251 where $\epsilon_t = 2.5 \times 10^{-7}/\beta\gamma$ m is the beam transverse emittance [15], and β_f
 252 is a beta-function near the cavity. Finally, we can rewrite:

$$\delta f \gg \frac{cx_0 \tilde{I}(R/Q)^{(1)}}{8\sqrt{2}\pi\beta\gamma U_0 \sqrt{\epsilon_t/\beta_f}}, \quad (7)$$

253 where U_0 is the proton mass in eV. The worst case corresponds to the begin-
 254 ning of HE 650 MHz section of Project-X linac, where the dipole mode has
 255 highest transverse shunt impedance ($f = 1376$ MHz, $(R/Q)^{(1)} = 60$ k Ω/m^2),

256 proton energy is 500 MeV ($\beta_f = 15$ m), the beam offset is 1 mm, the near-
 257 est beam spectrum line amplitude is 0.3 mA, and the resulting frequency
 258 detuning is $\delta f \gg 1$ Hz. When a dipole HOM is in exact resonance,

$$U_{kick} = \frac{x_0}{k} \frac{\tilde{I}}{2} (R/Q)^{(1)} Q_L. \quad (8)$$

259 Using this and Eq. 6 we estimate the maximum allowable value of the dipole
 260 HOM loaded quality factor to be $Q_L \ll 6 \times 10^8$. Typical value of Q_L in
 261 superconducting RF cavities is less (much less for the most HOMs) than 10^8 .
 262 Also, condition on δf can be satisfied by cavity spectrum manipulation (see
 263 Section 6). Therefore, the growth of the beam transverse emittance does not
 264 look to be a problem for the Project-X linac.

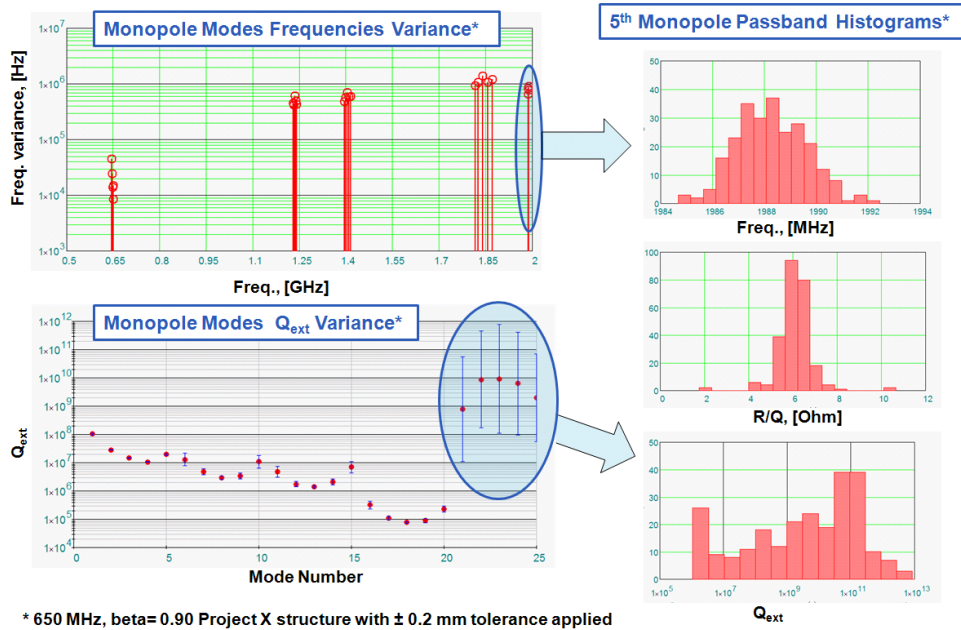


Figure 17: Variations of monopole HOMs parameters for the HE 650 MHz Project-X structure.

265 In order to accurately estimate the probability of resonance HOM exci-
 266 tation in the Project-X linac by one of the beam component, one has to do
 267 statistical analysis, which requires spread of the data for HOM parameters
 268 (frequency, impedance and quality factor). For the ILC cavity the r.m.s.
 269 spread σ_f of the resonance frequency is about 6–9 MHz depending on the

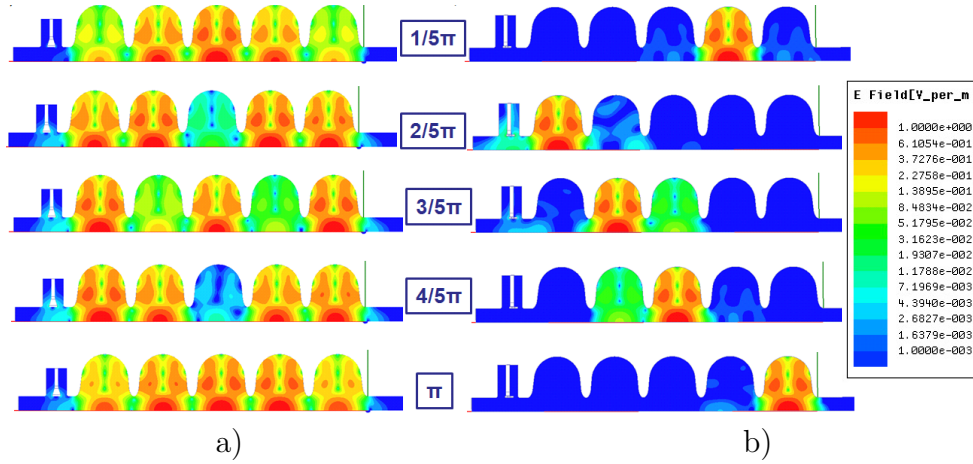


Figure 18: Electric fields distortion of the 5th monopole band for the HE 650 MHz Project-X structure; a) an ideal structure, b) a structure in presence of misalignments. In both cases the operating mode is tuned to correct frequency and field flatness.

pass-band, according to the DESY measurement statistics [16]. We do not have the experimental data available for Project-X linac yet. One way to obtain this information is to perform cavity HOM simulations taking into account manufacturing mechanical tolerances. Measurements of the profile of 1.3 GHz ILC cavity made in Cornell show that there are deviations from the ideal cavity of the order of ± 0.2 mm [17]. We take this value as a base for our statistical simulation of the Project-X HE 650 MHz structure. Geometrical parameters of the cavity individual half-cells (as shown in Table 5) allowed to randomly vary within ± 0.2 mm tolerances around standard values. While running the simulation with an imperfect cavity geometry, we tune the individual cell frequency by changing its length and preserving the field flatness of the accelerating mode along the cavity at the same time. Finally, we calculate HOM spectrum of the derived 5-cell structure, using HFSS code [18] with PEC boundary conditions at the beam pipe ends. Data are accumulated for further statistical analysis by repeating the simulation for multiple random structures. A typical result for the variations of monopole HOMs parameters is illustrated in Figure 17.

Besides the natural spread of the HOM parameters from cavity to cavity, random deviations of geometry from the designed shape due manufacturing tolerances in real cavity, may significantly change EM field distribution of

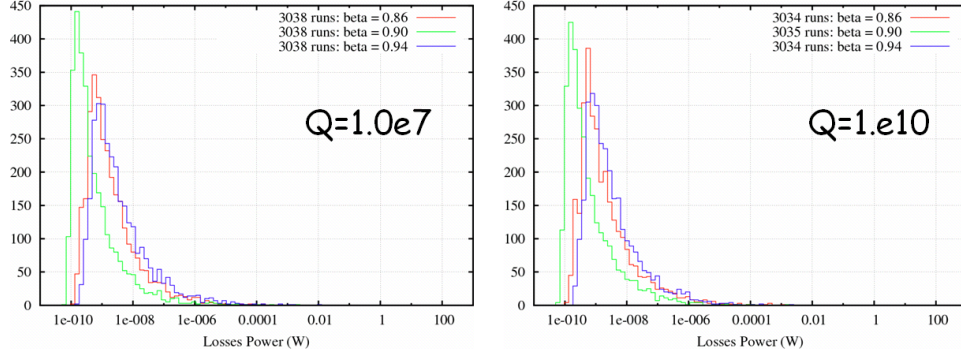


Figure 19: Calculations of the power losses in the HE 650 MHz cavities.

290 HOMs from a very narrow pass-band, when cell-to-cell coupling is very weak.⁹
 291 This effect is illustrated in Figure 18 for the 5th monopole pass-band of the
 292 HE 650 MHz Project-X cavity. Some of the modes, such as $\pi/5$, $3\pi/5$, and
 293 $4\pi/5$ in Figure 18b, become trapped in the internal cells of a cavity. Such
 294 a distortion causes (R/Q) and Q_L of an actual cavity to differ significantly
 295 from theoretical values.

296 By using the predicted deviations of monopole HOMs frequency, Q_L , and
 297 (R/Q) we generated 10^5 random linacs in order to estimate probability of
 298 the RF losses per cryomodule. The results of this computation for the HE
 299 650 MHz cavities are presented in Figure 19. The tail of these distributions
 300 in the region of a high power losses has only a weak dependence on the beam
 301 energy. Thus, we can neglect the effect of RF losses variation along the linac.
 302 The cumulative probability of losses per cryomodule is shown in Figure 20
 303 for three cases, when maximum, theoretical and actual (R/Q) values are
 304 taken into account. We can see from this plot, that the probability to have
 305 losses of 1 W is in the range 3×10^{-5} – 10^{-3} ; or, alternatively, the HOM power
 306 loss is in the range 0.01–1 W per cryomodule with a probability 10^{-3} . Our
 307 simulation also shows that main contribution in the region of high losses is
 308 due to trapped modes of the 5th pass-band.

⁹In this case, when geometry of individual cells vary across the cavity, coupling between cells is weak and also varies from cell to cell, the usual pass-band structure of N modes of $m\pi/N$ -kind, where N is number of cells and m runs from 1 to N ([2], Chapter 7), may change. The field of a mode may, for example, be concentrated in a single cell, or two adjacent cells.

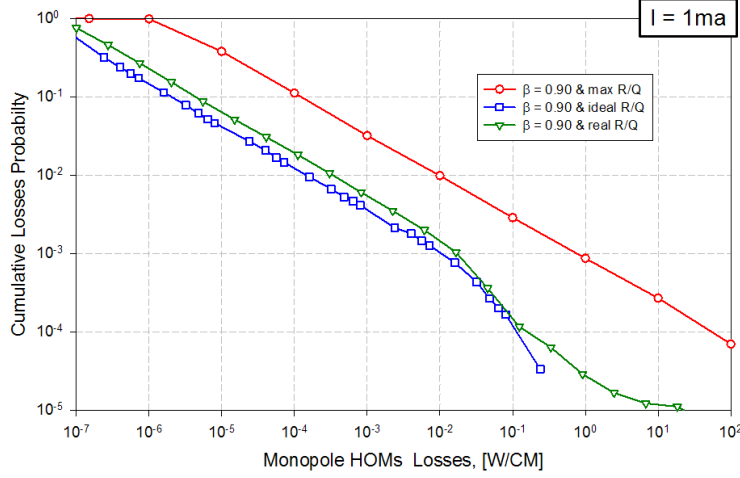


Figure 20: Probability of monopole HOMs power loss per cryomodule for the HE 650 MHz cavities of the Project-X linac; red is maximum (R/Q) w.r.t. the beam velocity for all HOMs; blue is theoretical (R/Q) for ideal cavity, and green is “realistic” (R/Q) for a cavity with mechanical errors.

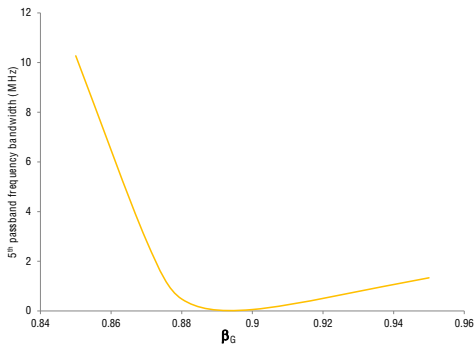
309 We may conclude that cryogenic losses due to resonant excitation of
 310 monopole HOM in HE 650 MHz structures is not a problem for the con-
 311 sidered Project-X parameters, CW regime and 1 mA average beam current.

312 *Operation of Project-X linac in a high beam current regime.* Possible future
 313 upgrades of Project-X may require to operate linac in a regime of a high beam
 314 current, when an average beam current is 5 mA or even 10 mA. As it has
 315 been discussed earlier in this section, monopole high order modes of the 5th
 316 pass-band of HE 650 MHz structure may become trapped in the internal cells
 317 of the cavity, leading to a high value of Q_L . This and the fact that cryogenic
 318 losses are proportional to square of the average beam current, $P_{loss} \sim I_{beam}^2$
 319 may potentially increase P_{cryo} up to hundred Watt for the 10 mA average
 320 beam current.

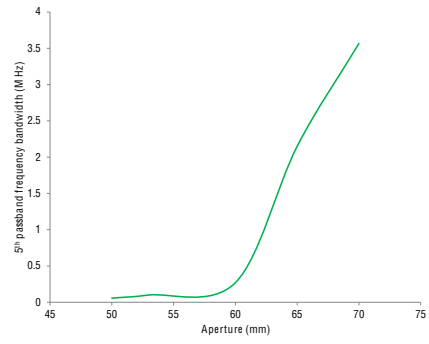
321 Figure 21 shows dependence of bandwidth of the 5th passband on geo-
 322 metrical beta (a) and aperture (b). An alternative design of elliptical cavity
 323 with a larger aperture (59 mm) and $\beta_G = 0.92$ is suggested for HE 650 MHz
 324 section in order to comply with various upgrade scenarios of the Project X
 325 linac [19]. Geometrical parameters of the cavity are shown in Table 6. We
 326 perform a similar statistical analysis of the HOM spectrum for this cavity.
 327 Figure 22 shows monopole HOM RF losses for the beam current of 1 mA and

Table 6: Geometrical parameters of alternative cavity design for HE 650 MHz section of Project X linac.

Dimension	$\beta_G = 0.92$	
	Regular Cell	End Cell
r , mm	59	59
R , mm	200.05	200.05
L , mm	97.56	106.08
A , mm	84	85
B , mm	90	78
a , mm	13	20
b , mm	28	33
α , $^\circ$	1.3	1.9



a)



b)

Figure 21: Dependence of the 5th pass-band bandwidth on geometrical beta, β_G (a) and aperture (b).

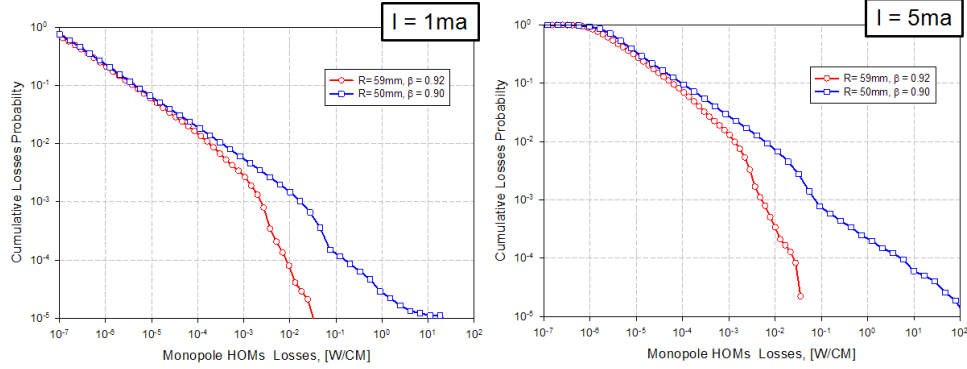


Figure 22: Probability of monopole HOMs RF losses per cryomodule for the present (blue) and alternative (red) version of HE 650 MHz cavities for Project-X.

5 mA for both present and alternative cavities. The new cavity shape suppresses high Q_L of the monopole HOM completely and mitigates the problem of large cryogenic losses.

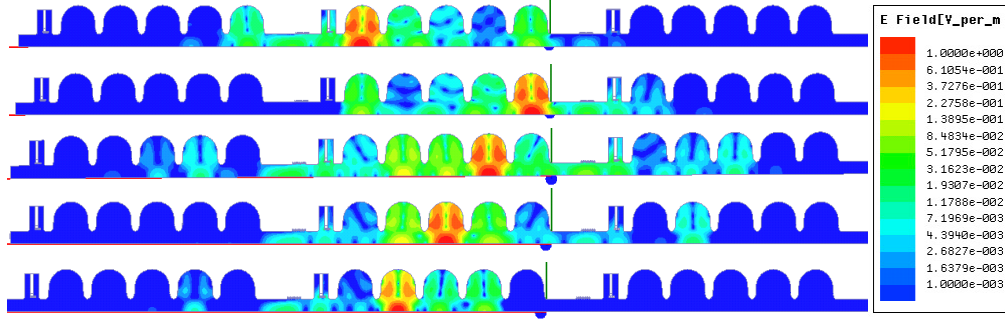


Figure 23: Field distribution for propagating monopole HOMs that are effectively trapped inside the cavity chain.

It is interesting to note, that in the alternative HE 650 MHz cavity with a larger aperture, monopole modes of the 5th pass-band have frequencies above the beam pipe cut-off frequency and become propagating modes. We perform simulation of RF field in a chain of three cavities interconnected with bellows, randomly varying geometry of cavities, as described above. We find solutions of our simulation where the field of the propagating HOMs is concentrated in the central cavity and the modes are effectively trapped inside the cavity chain. Figure 23 shows distribution of RF fields of trapped

339 HOMs.

340 5.1. Longitudinal emittance dilution

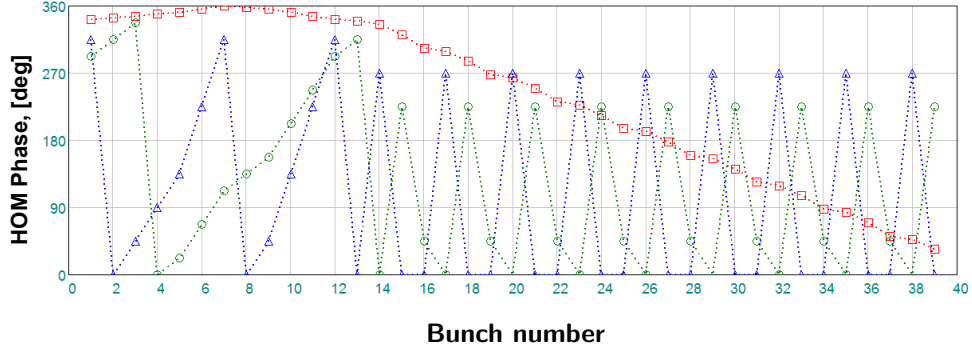


Figure 24: Resonance monopole HOM excitation in the HE 650 MHz structure broken up by various beam components (red is 1 MHz, green is 10 MHz, blue is 20 MHz).

341 Baseline Project-X design has a complicate beam structure that con-
 342 sists of three sub-components (1MHz, 10MHz, and 20MHz, see Figure 8).
 343 HOM frequencies are not harmonics of the frequencies of these beam sub-
 344 components. The phase of the voltage of an HOM excited by the resonance
 345 with one of the beam components is random with respect to two other com-
 346 ponents of the beam. The idea is illustrated in Figure 24. In case of a
 347 high- Q resonance, such an HOM may introduce a significant energy varia-
 348 tion along the beam train. This variation is proportional to the amplitude of
 349 the beam current spectrum line closest to the HOM frequency. Such effect
 350 is absent if the beam structure is regular and the beam spectrum consists of
 351 sub-harmonics of a single frequency.

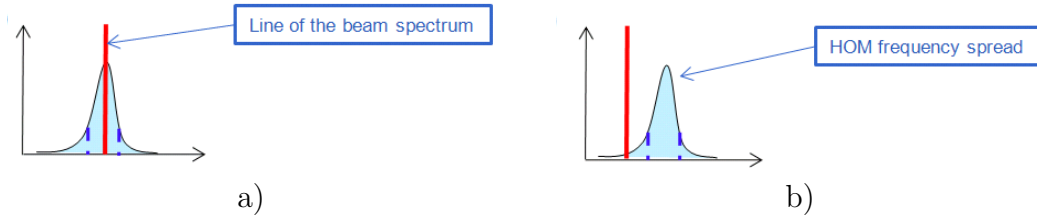


Figure 25: HOM excitation by beam sub-harmonic; a) - symmetrical and b) non - symmetrical options.

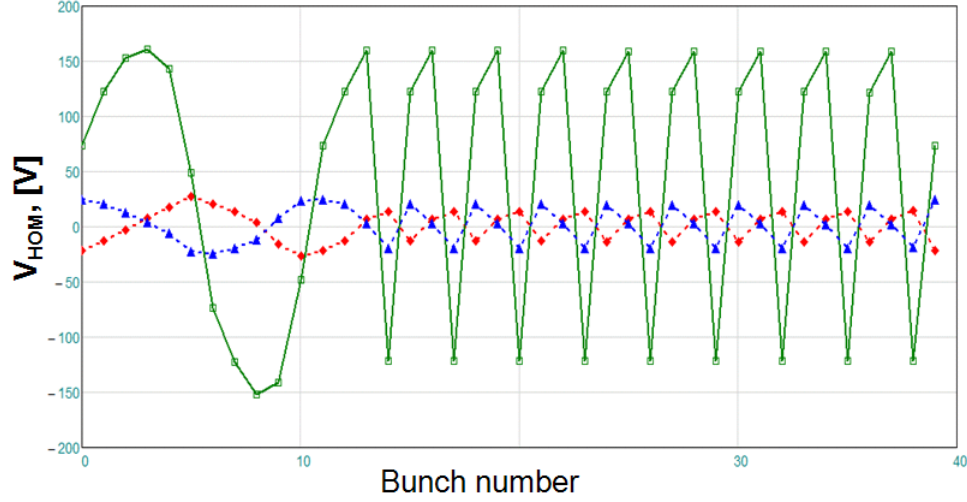


Figure 26: Monopole HOM ($I_{beam} = 1$ mA, $Q_L = 10^5$) excitation by the 10 MHz beam component, green curve — on resonance, read and blue — of resonance ($\pm 3\sigma$) excitations.

The width of a beam spectrum line is much more narrow compared to the spread of HOM frequencies. We consider two possible situations, when a beam line frequency is close to an HOM frequency:

1. symmetric, shown in Figure 25a, when a line in the beam spectrum coincides with the mean value of the HOM frequency distribution. By construction, this is unlikely situation. Energy spread along the bunch train does not increase as beam travels along linac.
2. non-symmetric, when the beam line frequency is shifted with respect to the HOM frequency (see Figure 25b). This is very probable situation. The energy spread caused by the HOMs excitation accumulates along the linac.

Figure 26 illustrates the principle of compensation (or accumulation) of the beam energy spread. The typical process of the longitudinal emittance growth is shown on Figure 27.

We perform a statistical analysis in order to calculate the probability of the beam longitudinal emittance growth as the following. We simulate 10^5 Project X linacs (HE 650 MHz section only) with random variation of HOM parameters (frequency, impedance, loaded quality factor) in cavities according to the model described earlier in this Section (see Figure 17). Energy

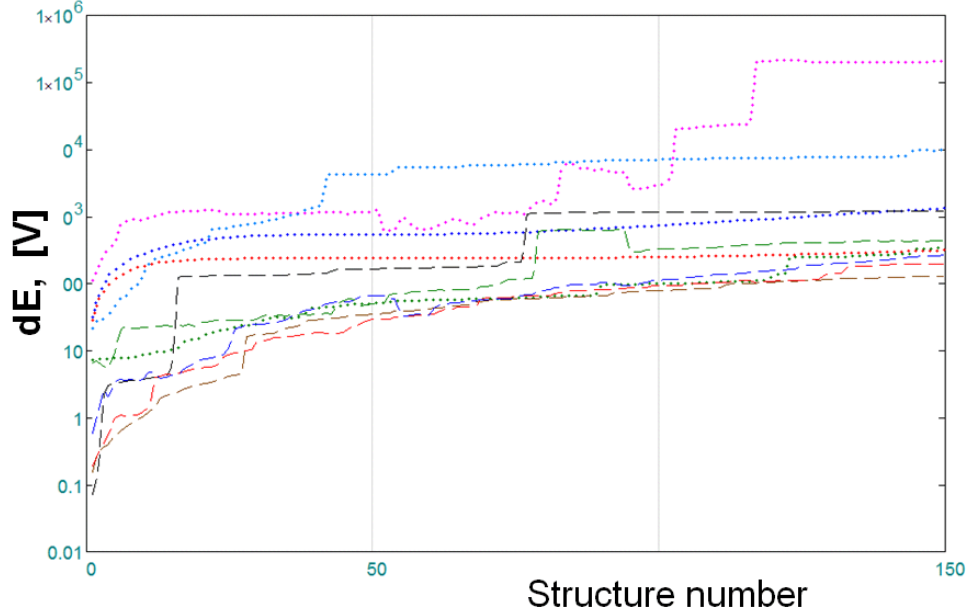


Figure 27: Growth of the energy spread in the beam train along the HE 650 MHz part of Project-X linac due to monopole HOMs excitations; dotted curves — 1st and 2nd passbands, dashed — 5th passband.

spread from bunch to bunch and longitudinal emittance growth are determined for every simulated linac. The results are summarized in Figure 28 and Figure 29 for 1 mA, 5 mA and 10 mA average beam currents. The simulation shows that the 2nd and 5th monopole passbands are the most dangerous and, thus, require a special care in order to avoid high- Q resonances.

6. Manipulation of HOM spectra

It is shown in the previous section, that the probability of one of the HOM of 650 MHz cavities to be in exact resonance with a line of beam current spectrum is small. In a rare case when it is happened, the following approach has been demonstrated to work [20]. HOM frequency can be moved by detuning cavity's accelerating mode by few tens of kHz and then tuning operating mode back to resonance.

A test, described in [20], was performed with 1.3 GHz 9-cell ILC cavity cooled to 2 K. The operating mode was detuned by 90 kHz and then tuned back. Because of small residual deformation of the cavity, HOM frequencies

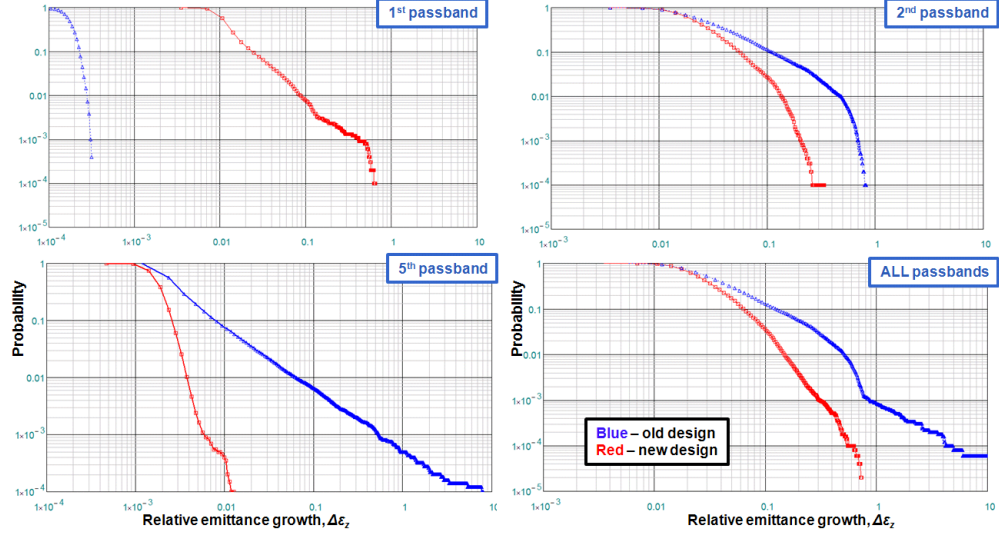


Figure 28: Probability of longitudinal emittance growth in the HE 650 MHz part of the Project-X linac for 1 mA average beam current. Data for the present design of the cavity are shown in blue, data for the alternative design are in red.

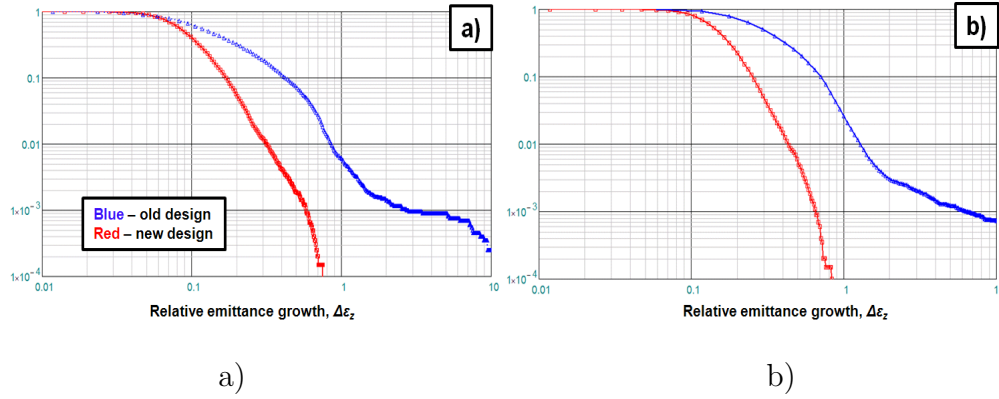


Figure 29: Probability of longitudinal emittance growth in the HE 650 MHz part of the Project-X linac for 5 mA (a) and 10 mA (b) average beam current. Data for the present design of the cavity are shown in blue, data for the alternative design are in red.

386 moved by 100–500 Hz after this procedure.

387 7. Collective beam effects

388 We study two types of collective beam effects caused by HOMs: beam
 389 breakup, affecting transverse beam dynamics; and longitudinal, klystron-type
 390 instabilities (see, for example, [21, 22]). In general, we do not expect the
 391 collective effects to be an issue, due to the following: 1) there is no feedback
 392 in linac as it is in circular accelerators, each bunch interacts with every cavity
 393 only once, resonance and amplification conditions can not be realized as in
 394 circular accelerator when bunches pass that same cavities multiple times; 2)
 395 we have few different types of cavities with different spectra, HOMs excited in
 396 one type of cavities do not affect excitation of HOMs in other types of cavities,
 397 since frequencies of these modes are uncorrelated; 3) there is spread of HOM
 398 frequencies in each cavity type, caused by manufacturing errors, thus, even if
 399 a certain HOM is in resonance condition in one cavity, it may be off resonance
 400 in other cavities; 4) HOM impedances depend on beam velocity, amplitudes
 401 of excited HOMs vary from cavity to cavity and can only reach the maximum
 402 possible value in few cavities, where the beam velocity is optimal for HOM
 403 excitation; 5) beam current is small, power loss to HOMs scales as square of
 404 beam current (Equation (4)), effects of HOMs on longitudinal and transverse
 405 beam dynamic are proportional to the beam current (Equations (2) and (5)).
 406 We focus our study of beam instabilities on 650 MHz section of Project X
 407 linac, the longest one with the highest beam velocity.

408 7.1. Transverse dynamics

409 We use a simplified model to investigate transverse beam dynamics in
 410 the field of dipole HOMs. We assume short bunches. We use lattice design
 411 as outlined in [23]. Five dipole passbands in LE and HE 650 MHz section
 412 are taken into account. Misalignment of cavities is random. Beam timing
 413 structure corresponds to 3 GeV program (Sec. 3, Figure 8). The deflecting
 414 gradient U'_{n+1} at the passage of bunch $n + 1$ through a cavity can be written
 415 as the following:

$$U'_{n+1} = U'_n e^{j\omega_{HOM}T - T/\tau} - \frac{1}{2}q_b R^{(1)}\omega_{HOM}(x - x_{cav}),$$

416 where q_b is the bunch charge, $R^{(1)} = Q_{ext}(R/Q)^{(1)}$ is the dipole mode impe-
 417 dance, x and x_{cav} are the beam and cavity offsets. Then, change of the bunch

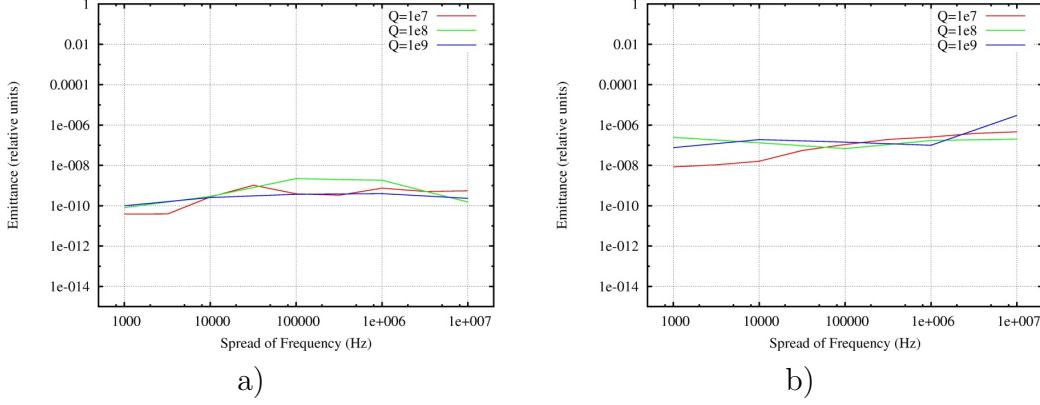


Figure 30: Transverse (a) and longitudinal (b) emittance dilution as a function of HOM frequency spread.

transverse momentum is

$$\Delta p_{\perp} = \Re \left(j \frac{\beta}{\omega} U' \right).$$

We run simulation for 1 mA average beam current and 0.5 mm R.M.S. of random transverse offsets of cavities. Results of simulation are shown in Figure 30 (left). One can see, that the variations of the transverse emittance are negligible in the wide range of HOM frequency spread and Q_{ext} .

7.2. Longitudinal instability

Similarly, we estimate effect of longitudinal HOMs on the longitudinal beam dynamics (the so-called “klystron-type” instability). Figure 30 (right) shows results of this simulation. Again, no noticeable changes in longitudinal emittance are observed.

8. Discussion and conclusion

8.1. Comparison to SNS

SNS is successfully operated superconducting proton linac. It has two ($\beta = 0.61$ and $\beta = 0.81$) sections of elliptical 6-cell 805 MHz cavities. We benchmark our simulation of HOM power loss in 650 MHz sections of Project-X linac against SNS. Figure 31 shows comparison of power loss due to resonance excitation of monopole HOM for Project-X HE 650 MHz and SNS $\beta = 0.81$ 805 MHz cavities. One can see, that expected HOM power

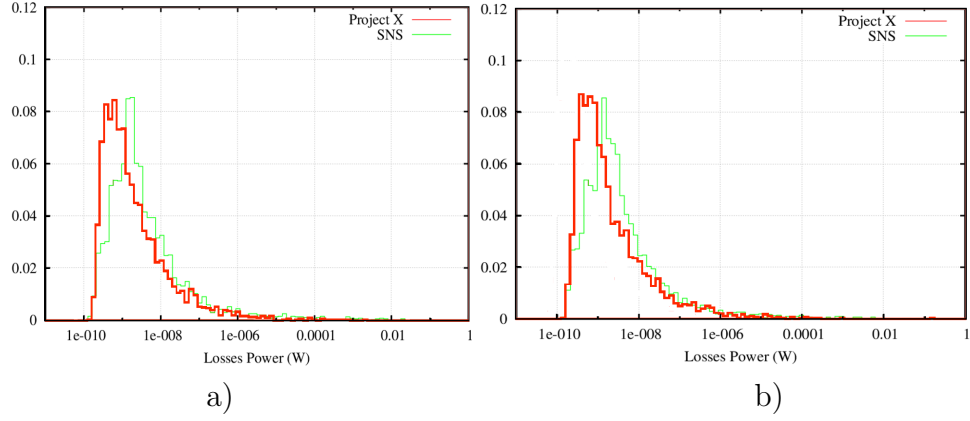


Figure 31: Distribution of power loss per cavity for Project-X HE 650 MHz and SNS $\beta = 0.81$ 805 MHz cavities. (a) $Q_L = 10^8$, (b) $Q_L = 10^9$.

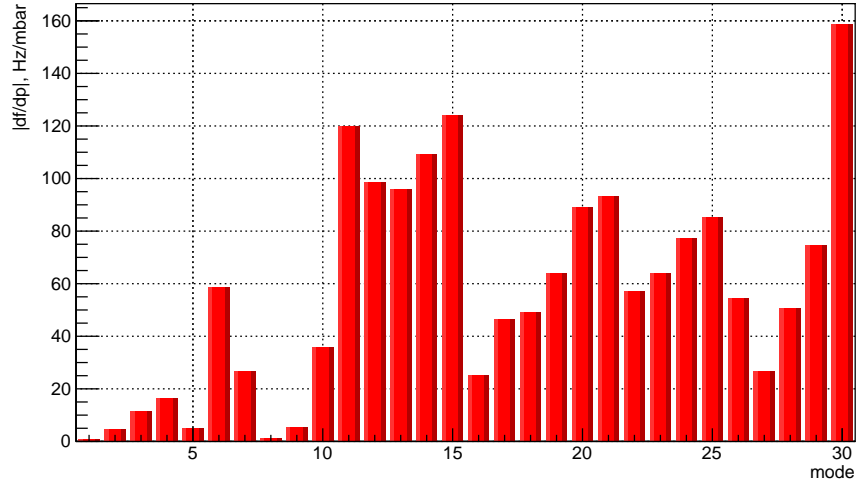


Figure 32: Microphonics for the monopole HOM in HE 650 MHz cavity.

loss in Project-X is smaller than in SNS linac, which is already quite small. Since SNS operates in pulsed regime, Lorentz force detuning of cavities during pulses and pulse-to-pulse jitter reduce HOM power loss even more. In Project-X linac, which operates in CW regime, similar effect of reduction of HOM losses may be expected from microphonics. Figure 32 shows sensitivity of the monopole HOMs frequencies to the variations of pressure in liquid Helium bath for HE 650 MHz cavity. Cavity and Helium vessel are optimized in order to minimize effect of microphonics for operating mode. High order modes have larger detuning due to pressure variations, which is increasing with the mode frequency. Relatively large frequency variations of HOMs due to microphonics reduce probability of resonance excitation and detune HOMs from resonance if resonance conditions happen.

8.2. Conclusion

We study effects of high order modes in Project-X superconducting CW linac. The main goal of this study is to answer the question of whether HOM couplers/dampers are needed or not in SRF accelerating cavities of Project-X. Multiple issues related to the excitation of HOMs and their adverse effect on cryogenic losses and beam dynamics are addressed.

We find that beam breakup and “klystron”-type instabilities are negligible in 650 MHz section of the linac. Incoherent HOM losses are small. Resonance excitation of dipole modes does not look to be an issue. Accidental resonance excitation of the monopole modes in HE 650 MHz section may lead to the longitudinal emittance dilution, but the probability is small and HOM frequency can be moved from the dangerous resonance condition by detuning cavity operating mode and then tuning it back.

Based on this study we conclude that HOM couplers and dampers are not needed in Project-X linac.

References

- [1] <http://projectx.fnal.gov/>
- [2] H. Padamsee, J. Knobloch and T. Hays, *RF Superconductivity for Accelerators*, Wiley, New York, 1998.
- [3] F. Marhauser *et al.*, *Design, fabrication and testing of medium-beta 650 MHz cavity prototypes for Project-X*, IPAC 2011, San Sebastian, Spain, September 4–9, 2011.

- 470 [4] V. Yakovlev *et al.*, *Concept EM design of the 650 MHz cavities for the*
471 *Project X*, PAC 2011, New York, NY, USA, March 28–April 1, 2011.
- 472 [5] S.-H. Kim, *SNS SCL Experiences*, Project-X Collaboration Meeting,
473 ORNL, Tennessee, USA, April 12–14, 2011.
- 474 [6] J. Sekutowicz, *HOM couplers at DESY*, HOM Workshop, Cornell Uni-
475 versity, Ithaca, New York, USA, October 11–13, 2010.
- 476 [7] D. G. Myakishev, V. P. Yakovlev, *The New Possibilities of SuperLANS*
477 *Code for Evaluation of Axisymmetric Cavities*, PAC 1995, Dallas, Texas,
478 USA, May 1–5, 1995.
- 479 [8] ILC Reference Design Report,
480 [http://www.linearcollider.org/about/](http://www.linearcollider.org/about/Publications/Reference-Design-Report)
481 [Publications/Reference-Design-Report](http://www.linearcollider.org/about/Publications/Reference-Design-Report)
- 482 [9] <http://xfel.desy.de/>
- 483 [10] J. N. Corlett, *et al.*, *A Next Generation Light Source Facility at LBNL*,
484 PAC 2011, New York, NY, USA, March 28–April 1, 2011.
- 485 [11] A. Lunin, V. Yakovlev, S. Kazakov, *Cavity loss factors of non-relativistic*
486 *beams for Project X*, PAC 2011, New York, NY, USA, March 28–April
487 1, 2011, TUP075.
- 488 [12] <http://www.cst.com/>
- 489 [13] M. H. Awida, P. Berrutti, I. V. Gonin, T. N. Khabiboulline, V. P.
490 Yakovlev, *SSR1 HOM Analysis and Measurements*, IPAC 2012, New
491 Orleans, Louisiana, USA, May 20–25, 2012.
- 492 [14] J. C. Slater, *Microwave Electronics*, D. Van Nostrand, Princeton, 1950.
- 493 [15] N. Solyak, J-P. Carneiro, V. Lebedev, S. Nagaitsev, N. Perunov, J-F.
494 Ostiguy, A. Vostrikov, V. Yakovlev, *Design of the Project X CW Linac*,
495 LINAC 2010, Tsukuba, Japan, September 12–17, 2010.
- 496 [16] J. Sekutowicz, *HOM damping*, ILC Workshop, KEK, Japan, November
497 13–15, 2004.

- 498 [17] R. Sundelin, *Frequency Spreads Caused By Manufacturing Tolerances*,
499 Cornell CLNS internal note SRF-830102-EXA, 1983.
- 500 [18] ANSYS HFSS, <http://www.ansys.com/hfss>
- 501 [19] A. Lunin, A. Saini, A. Sukhanov, N. Solyak, V. Yakovlev, *Alternative*
502 *Cavity for the HE Part of the Project X Linac*, IPAC 2012, New Orleans,
503 Louisiana, USA, May 20–25, 2012.
- 504 [20] T. Khabiboulline, *Experiments on HOM Spectrum Manipulation in a*
505 *ILC 1.3 GHz Cavity*, HOM Workshop, Cornell University, Ithaca, New
506 York, USA, October 11–13, 2010.
- 507 [21] J. Tuckmantel, *Do we need HOM dampers on superconducting cavities*
508 *in proton linacs?*, HOM Workshop, CERN, Switzerland, June 25–26,
509 2009.
- 510 [22] M. Schuh, F. Gerigk, J. Tuckmantel, C.P. Welsch, *Higher order mode*
511 *analysis of the SPL cavities*, IPAC 2010, Kyoto, Japan, May 23–28,
512 2010.
- 513 [23] J.-F. Ostiguy, P. Berrutti, J.-P. Carneiro, V. A. Lebedev, S. Nagaitsev,
514 A. Saini, B. G. Shteynas, N. Solyak, V.P. Yakovlev, *Status of the Project-*
515 *X CW Linac Design*, IPAC 2012, New Orleans, Louisiana, USA, May
516 20–25, 2012.